Article

Why Are MgC₃H Isomers Missing in the Interstellar Medium?

Sunanda Panda, Devipriya Sivadasan, Nisha Job, Aland Sinjari, Krishnan Thirumoorthy, Anakuthil Anoop, and Venkatesan S. Thimmakondu*

Cite This: *J. Phys. Chem. A* 2022, 126, 4465−4475

Read Online

| ACCESS | | Metrics & More | | Article Recommendations | | Supporting Information |

ABSTRACT: Considering the recent findings of linear doublet ($^2\Sigma^+$) MgC$_n$H isomers (n = 2, 4, and 6) in the evolved carbon star IRC+10216, various structural isomers of MgC$_3$H and MgC$_3$H$^+$ are theoretically investigated here. For MgC$_3$H, 11 doublet and 8 quartet stationary points ranging from 0.0 to 71.8 and 0.0 to 110.1 kcal mol^{-1}, respectively, have been identified initially at the UωB97XD/6-311++G(2d,2p) level. To get accurate relative energies, further energy evaluations are carried out for all isomers with coupled cluster methods and thermochemical modules such as G3//B3LYP, G4MP2, and CBS-QB3 methods. Unlike the even series, where the global minima are linear molecules with a Mg atom at one end, in the case of MgC$_3$H, the global minimum geometry turns out to be a cyclic isomer, 2-magnesabicyclo[1.1.0]but-1,3,4-triyl (**1**, C_{2v}, $^2A_1$). In addition, five low-lying isomers, magnesium-substituted cyclopropenylidene (**2**, C_s, $^2A'$), 1-magnesabut-2,3-dien-1-yl-4-ylidene (**3**, C_s, $^2A''$), 1-magnesabut-2-yn-1-yl-4-ylidene (**4**, C_s, $^2A''$),

$2\lambda^3$-magnesabicyclo[1.1.0]but-1,3-diyl-4-ylidene (**5**, C_{2v}, $^2A_1$), and 1-magnesabut-2,3-dien-2-yl-4-ylidene (**6**, $C_{\infty v}$, $^2\Sigma^+$), were also identified. The doublet linear isomer of MgC$_3$H, 1-magnesabutatrienyl (**10**, $C_{\infty v}$, $^2\Sigma^+$) turns out to be a minimum but lies 54.1 kcal mol^{-1} above **1** at the ROCCSD(T)/cc-pVTZ level. The quartet ($^4\Sigma^+$) electronic state of **10** was also found to be a minimum, but it lies 8.0 kcal mol^{-1} above **1** at the same level. Among quartets, isomer **10** is the most stable molecule. The next quartet electronic state (of isomer **11**) is 34.4 kcal mol^{-1} above **10**, and all other quartet electronic states of other isomers are not energetically close to low-lying doublet isomers **2** to **6**. Overall, the chemical space of MgC$_3$H contains more cyclic isomers (**1**, **2**, and **3**) on the low-energy side unlike their even-numbered MgC$_n$H counterparts (n = 2, 4, and 6). Though the quartet electronic state of **10** is linear, it is not the global minimum geometry on the MgC$_3$H potential energy surface. Isomerization pathways among the low-lying isomers (doublets of **1**−**4** and a quartet of **10**) reveal that these molecules are kinetically stable. For the cation, MgC$_3$H$^+$, the cyclic isomers (**1$^+$**, **2$^+$**, and **3$^+$**) are on the low-energy side. The singlet linear isomer, **10$^+$**, is a fourth-order saddle point. The low-lying cations are quite polar, with dipole moment values of >7.00 D. The current theoretical data would be helpful to both laboratory astrophysicists and radioastronomers for further studies on the MgC$_3$H$^{0/+}$ isomers.

■ INTRODUCTION

Finding molecules many light years away is not only an open challenge to the scientific community but also an essential study that needs to be undertaken for a thorough understanding of star-forming regions, the formation of planets, and astrobiology.[1−9] To confirm the molecules in an unambiguous manner in the interstellar medium (ISM) and circumstellar shells, laboratory rest frequencies are an essential prerequisite in most cases.[10−23] Therefore, logically analyzing astrochemical issues requires a coordinated effort from experts across the scientific community, which includes radioastronomers, astrophysicists, molecular spectroscopists, organic chemists, electrical engineers, and quantum information scientists.[24−33] As an example, let us take the case of a linear MgC$_2$H radical. The pure rotational spectrum of 1-magnesaprop-2-yn-1-yl (MgC$_2$H, $^2\Sigma^+$) was recorded by Ziuyrs and co-workers in 1995.[34,35] It was speculated at that time that MgC$_2$H would be present in the ISM because it is isoelectronic with MgNC[36] and MgCN.[37] Through ab initio calculations, Woon suggested

the formation pathways of MgC$_2$H, MgC$_2$H$^+$, and cyclic-MgC$_2$ in the ISM.[38,39] Nearly two decades later, MgC$_2$H was tentatively assigned in the evolved carbon star, IRC+10216, in 2014.[40] Five years later, in 2019, the presence of MgC$_2$H was finally confirmed along with the findings of MgC$_4$H and MgC$_3$N.[41] It is noted here that the confirmation of MgNC ($^2\Sigma^+$) in IRC+10216 triggered interest in this molecule as well as in other organomagnesium compounds.[42−48] MgNC has also been identified in two protoplanetary nebulae, CRL 2688 and CRL 618.[49,50] The metastable isomer of the MgNC radical, MgCN, was also confirmed in IRC+10216 in 1995.[37] In 2021, the presence of MgC$_6$H (1-magnesahept-2,4,6-triyn-
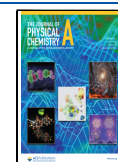
1-yl) was also confirmed.[51] Naturally, these observations consequently provoke a question regarding the presence of odd series of MgC_nH isomers (where, $n = 3, 5, 7$, etc.,) in IRC +10216 and/or in other interstellar sources. Thus, in this work, we have theoretically characterized the potential energy surfaces of MgC_3H and MgC_3H^+ using density functional theory and coupled-cluster methods.

Though several experimental studies have been carried out to record the electronic transitions of $MgC_{2n}H$ ($n = 1-3$) in the visible region (in the gas phase),[52−55] the number of experimental studies for the odd series $MgC_{2n-1}H$ ($n \geq 2$) appears to be limited. In the past, Largo and co-workers carried out theoretical studies for MgC_3 and MgC_3H^+ isomers at the MP2(full)/6-311G(d) and B3LYP/6-311G(d) levels.[56,57] Dong et al. have observed a great number of magnesium carbon hydride clusters ($Mg_mC_nH_x$) by the ablation of Mg foil into a mixture of 10% CH_4/He expansion gas in their mass spectra.[58] Notably, in their experiments, clusters with odd mass numbers (that is, systems containing an odd number of electrons) are detected, and no signal related to MgC_3H isomers was observed.[58] Graham and co-workers have recorded the vibrational spectrum of the linear MgC_3^- anion using Fourier transform infrared (FTIR) spectroscopy.[59]

Theoretical studies including structures, energetics, and spectroscopic properties of MgC_3H isomers have been missing until now in the literature. Thus, isomers of MgC_3H in their doublet and quartet electronic states (Figures 1 and 2) are
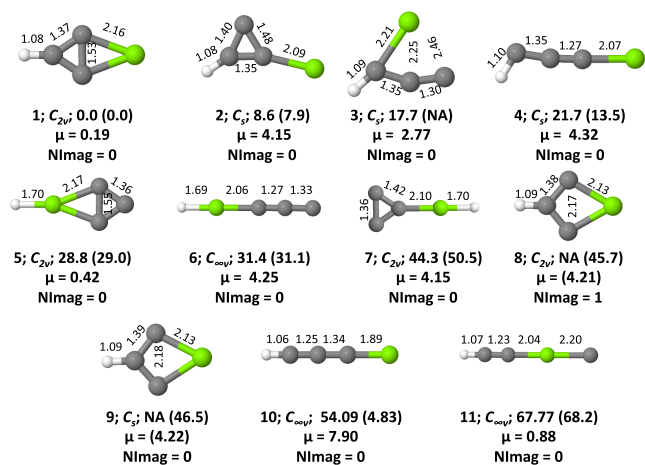

Figure 1. Isomers **1−11** of MgC_3H in their doublet ground electronic states. Relative energies (ZPVE inclusive, in kcal mol^{-1}) and dipole moments (in Debye) are calculated at the ROCCSD(T)/cc-pVTZ level. Values shown in parentheses are calculated at the CBS-QB3 level. The number of imaginary frequencies (NImag) obtained for each geometry is also given. Here, NA stands for not applicable, which means that the geometry either did not converge or led to some other geometry at that particular level.

characterized for the first time in this work. Six low-lying doublet isomers, 2-magnesabicyclo[1.1.0]but-1,3,4-triyl (**1**), magnesium-substituted cyclopropenylidene (**2**), 1-magnesa-but-2,3-dien-1-yl-4-ylidene (**3**), 1-magnesabut-2-yn-1-yl-4-yli-dene (**4**), $2\lambda^3$-magnesabicyclo[1.1.0]but-1,3-diyl-4-ylidene (**5**), and 1-magnesabut-2,3-dien-2-yl-4-ylidene (**6**), and one low-lying quartet isomer, 1-magnesabutatrienyl (**10**), could be considered to be suitable target molecules for experimental observations. Unlike the MgC_nH (where, $n = 2, 4, 6$, etc.) even series, where the global minima are linear molecules with the
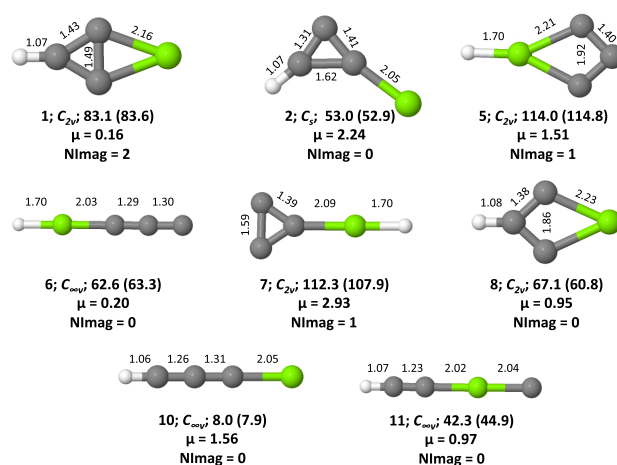

Figure 2. Isomers **1−11** of MgC_3H in their quartet ground electronic states. Relative energies (ZPVE inclusive, in kcal mol^{-1}) and dipole moments (in Debye) are calculated at the ROCCSD(T)/cc-pVTZ level. Values shown in parentheses are calculated at the CBS-QB3 level. The number of imaginary frequencies (NImag) obtained for each geometry is also given.

magnesium atom at one end, here for MgC_3H, a cyclic isomer (**1**) was identified to be the global minimum geometry. Considering the presence of Mg^+ and C_3H (both prop-1-yn-3-ylidyne and cycloprop-1-yn-3-yl) radicals in the ISM,[60−65] it is anticipated that isomers of MgC_3H could also be present. However, the prerequisite for detecting these molecules many light years away is the availability of laboratory rest frequencies,[66−74] but there appear to be no laboratory astrophysical studies for this system at the moment. Thus, computational studies are undertaken, which may aid not only the laboratory studies but also the radioastronomical observations.

■ COMPUTATIONAL DETAILS

For the doublet and quartet electronic states of MgC_3H and also for the triplet electronic states of MgC_3H^+, the geometry optimization calculations are initially carried out at the UωB97XD[75]/6-311++G(2d,2p)[76,77] level. For the singlet electronic states of MgC_3H^+, calculations are made at the same level using restricted Hartree−Fock (RHF) wave functions. Vibrational frequencies (harmonic) are calculated for each stationary point to confirm whether it is a minimum, transition state, or nth-order saddle point. The number of imaginary frequencies (NImag) obtained for each stationary point is indicated underneath the geometry. To obtain better relative energies, single-point energy calculations are carried out using the coupled-cluster (CC) method at either the UCCSD(T)[78,79]/6-311++G(2d,2p) or RCCSD(T)/6-311+ +G(2d,2p)/ωB97XD[75]/6-311++G(2d,2p) level on top of the optimized geometries obtained from density functional theory (DFT). The ωB97XD functional has been purposefully chosen because it incorporates empirical dispersion corrections[80] as well as long-range corrections. Full geometry optimization and frequency calculations for all MgC_3H isomers (doublets and quartets) are also carried out at the ROCCSD(T)/cc-pVTZ level. To further evaluate the relative energies, calculations are made using the composite methods, G3//B3LYP,[81] G4-(MP2),[82,83] and CBS-QB3.[84,85] These relative energies are

Table 1. ZPVE-Corrected Relative Energies of MgC$_3$H Isomers in their Doublet and Quartet Ground Electronic States Calculated at Different Levels

	doublets										
	1	2	3	4	5	6	7	8	9	10	11
level	$^2A_1$	$^2A'$	$^2A'$	$^2A''$	$^2A_1$	$^2\Sigma^+$	$^2A_1$	$^2A_1$	$^2A'$	$^2\Sigma^+$	$^2\Sigma^+$
ROωB97XD/6-311++G(2d,2p)	0.0	6.9	28.0[d]	30.2	30.3	34.5	51.0	b	b	32.1	72.6
UωB97XD/6-311++G(2d,2p)	0.0	6.8	25.6[d]	28.1	29.1	32.3	49.6	52.5	52.8	54.1	71.8
UCCSD(T)/6-311++G(2d,2p)[a]	0.0	8.1	27.0[d]	14.3	31.9	33.1	55.3	49.4	49.4	54.2	65.2
G3//B3LYP	0.0	7.9	c	17.7	29.2	30.1	50.8	50.8	52.5	8.7[e]	66.2
G4MP2	0.0	7.8	c	18.5	29.2	33.2	51.1	51.4	52.1	59.8	68.1
ROCCSD(T)/cc-pVTZ	0.0	8.6	17.7	21.7	28.8	31.7	50.9	b	b	54.1	68.5
CBS-QB3	0.0	7.9	c	13.5	29.0	31.1	50.5	45.7	46.5	4.8[f]	68.2
	quartets										
	1	2	3	4	5	6	7	8	9	10	11
level	$^4B_1$	$^4A''$			$^4A_2$	$^4\Sigma^+$	$^4B_1$	$^4A_2$		$^4\Sigma^+$	$^4\Sigma^+$
ROωB97XD/6-311++G(2d,2p)	87.5	54.0	c	c	120.7	69.3	118.7	63.5	g	13.1	47.5
UωB97XD/6-311++G(2d,2p)	85.0	51.4	c	c	116.2	61.0	107.9	58.8	g	6.1	46.4
UCCSD(T)/6-311++G(2d,2p)[a]	86.1	53.9	c	c	117.4	63.1	111.4	60.5	g	8.3	38.8
G3//B3LYP	83.0	52.3	c	c	113.5	62.2	107.3	60.7	g	6.6	41.5
G4MP2	84.3	54.3	c	c	116.4	67.0	110.0	63.0	g	10.9	45.6
ROCCSD(T)/cc-pVTZ	83.1	53.0	c	c	114.0	62.6	112.3	67.1	g	8.0	42.3
CBS-QB3	83.6	52.9	c	c	114.8	63.3	107.9	60.8	g	7.9	44.9

[a]Calculated at the UCCSD(T)/6-311++G(2d,2p)//UωB97XD/6-311++G(2d,2p) level. [b]Geometry optimization at this level for isomer **8** or **9** leads to isomer **1**. [c]Geometry optimization at this level for isomer **3** or **4** leads to isomer **10**. [d]The electronic state is $^2A''$. [e]The wave function is highly spin-contaminated ($\langle S^2 \rangle$ = 1.799861) at this level, and thus the relative energies are not in order. [f]The wave function is highly spin-contaminated ($\langle S^2 \rangle$ = 1.796338) at this level, and thus the relative energies are not in order. [g]Geometry optimization at this level for isomer **9** leads to isomer **8**.

Table 2. ZPVE-Corrected Relative Energies of MgC$_3$H$^+$ Isomers in their Singlet and Triplet Ground Electronic States Calculated at Different Levels

	singlets										
level	1	2	3	4	5	6	7	8	9	10	11
ωB97XD/6-311++G(2d,2p)	0.0	16.0	22.4	29.6	78.4	62.6	89.3	b	b	35.2	123.1
CCSD(T)/6-311++G(2d,2p)[a]	0.0	15.4	19.0	21.6	71.9	52.8	81.2	b	b	35.2	108.1
G3//B3LYP	0.0	14.7	19.3	19.0	70.7	51.6	80.6	b	b	33.7	110.6
G4MP2	0.0	14.2	19.7	18.3	69.1	52.4	80.5	b	b	35.2	111.0
CCSD(T)/cc-pVTZ	0.0	15.6	19.6	21.4	70.0	52.3	80.6	b	b	33.4	110.4
CBS-QB3	0.0	15.7	20.7	21.2	72.8	54.8	83.6	b	b	35.1	112.6
	triplets										
	1	2	3	4	5	6	7	8	9	10	11
level											
UωB97XD/6-311++G(2d,2p)	47.8	25.2	c	c	97.4	98.7	81.5	53.4		11.3	99.2
UCCSD(T)/6-311++G(2d,2p)[a]	47.2	23.3	c	c	96.6	95.6	80.8	54.7		13.7	87.9
G3//B3LYP	47.2	25.1	c	13.2	103.1	95.2	79.3	55.0		13.7	93.5
G4MP2	46.6	24.7	c	15.5	102.6	98.3	78.8	55.8		17.3	94.7
CBS-QB3	48.7	26.9	c	13.5	103.8	97.1	130.7	55.3		14.7	96.9

[a]Calculated at the (U)CCSD(T)/6-311++G(2d,2p)//(U)ωB97XD/6-311++G(2d,2p) level. [b]Geometry optimization at this level for isomer **8** or **9** leads to isomer **1**. [c]Geometry optimization at this level for isomer **3** or **4** leads to isomer **10**.

documented in Tables 1 and 2 for MgC$_3$H and MgC$_3$H$^+$ isomers, respectively.

For the low-lying doublet isomers, appropriate transition states have been identified at the UωB97XD/6-311++G-(2d,2p) level, and isomerization pathways were confirmed through intrinsic reaction coordinate (IRC)[86,87] calculations at the same level. To accurately determine the activation energy barriers, single-point energy calculations were made at the UCCSD(T)/6-311++G(2d,2p)//UωB97XD/6-311++G-(2d,2p) level. To assess the multireference character, T_1 diagnostic values[88] have been calculated at the UCCSD/6-311++G(2d,2p)//UωB97XD/6-311++G(2d,2p) level of

theory. To check the kinetic stability of isomers **1** ($^2A_1$) and **10** ($^4\Sigma^+$), *ab initio* molecular dynamics (AIMD) simulations using the atom-centered density matrix propagation (ADMP)[89] method are carried out at the UωB97XD/6-311++G(2d,2p) level of theory. All DFT calculations, calculations that involve composite methods, and AIMD simulations are carried out with the Gaussian suite of programs.[90] All coupled-cluster calculations have been carried out with the CFOUR (2.00 beta version) program package.[91]

■ RESULTS AND DISCUSSION

Optimized structures of isomers **1−11** of $MgC_3H^{0/+}$ in doublet, quartet, and singlet electronic states are shown in Figures 1, 2, and 3, respectively. For brevity, triplet electronic
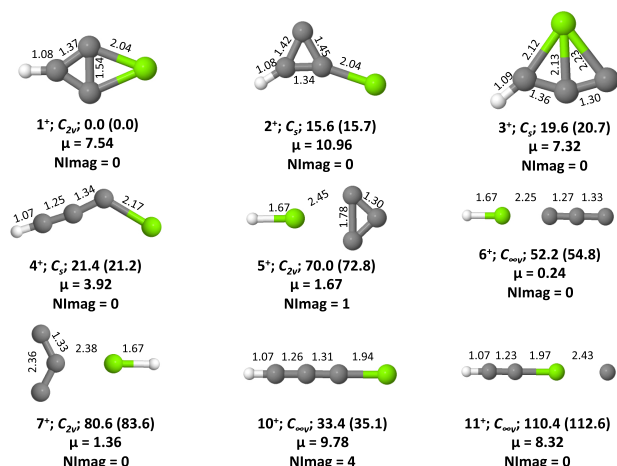

Figure 3. Isomers **1−11** of MgC_3H^+ in their singlet ground electronic states. ZPVE-corrected relative energies (in kcal mol^{-1}) and dipole moments (in Debye) are calculated at the CCSD(T)/cc-pVTZ level. Values in parentheses are calculated at the CBS-QB3 level. The number of imaginary frequencies (NImag) obtained for each geometry is also given.

states of MgC_3H^+ are not shown here because all of them energetically lie above singlets. Zero-point vibrational energy (ZPVE)-corrected relative energies obtained at various levels for MgC_3H and MgC_3H^+ isomers are shown in Tables 1 and 2,

respectively. Various spectroscopic parameters of isomers **1**, **10**, and **2** are collected in Tables 3, 4, and 5, respectively.

Energetics. *MgC_3H.* After analyzing the doublet and quartet electronic states of various isomers of MgC_3H, one could arrive at a conclusion that the doublet electronic state ($^2A_1$) of 2-magnesabicyclo[1.1.0]but-1,3,4-triyl (**1**) is the most stable isomer at various levels (see Table 1). From the energetic perspective, the first six isomers of the doublet (**1−6**) and the quartet of isomer **10** lie within 1.5 eV (∼34.6 kcal mol^{-1}). Therefore, the possibility of finding these molecules in the laboratory is quite high. Among the doublets, isomers **1** (μ = 0.19 D) and **5** (μ = 0.42 D) are less polar whereas **2**, **3**, **4**, and **6** are quite polar, with dipole moment values of 4.15, 2.77, 4.32, and 4.25 D, respectively. Isomer **10** of the quartet is also moderately polar (μ = 1.56 D). Though the doublet of **10** is highly polar (μ = 7.90 D), it lies 54.1 kcal mol^{-1} above **1** at the ROCCSD(T)/cc-pVTZ level. It is noted here that the relative energies obtained with respect to G3//B3LYP and CBS-QB3 methods for the doublet electronic state of isomer **10** are not in good agreement compared with other methods (see Table 1). The reason for this discrepancy is due to a large amount of spin contamination in both the G3//B3LYP and CBS-QB3 methods. Both methods use the UB3LYP functional for the geometry optimization. Ideally, for a doublet electronic state, the $\langle S^2 \rangle$ value should be 0.75. However, the values we obtained for isomer **10** were 1.799861 and 1.796338, respectively. The initial wave function is certainly very badly spin-contaminated; consequently, the energies are not in the correct order compared to other levels. We did do a stability analysis of the optimized geometries of **10** obtained through the G3//B3LYP and CBS-QB3 methods.[92] It is noted here that the wave functions are symmetry-broken and show UHF instabilities.[93] For these reasons, the energies reported with respect to the G3//B3LYP and CBS-QB3 methods for isomer

Table 3. Inertial Axis Dipole Moment Components, Absolute Dipole Moment (in Debye), Rotational and Centrifugal Distortion Constants (in MHz), Harmonic Vibrational Frequencies (in cm^{-1}), and IR Intensities (Given in Parentheses, in km mol^{-1}) of the $^2A_1$ Electronic State of Isomer 1 Calculated at Different Levels[a]

	6-311++G(2d,2p)		cc-pVTZ		
parameter	ROωB97XD	UωB97XD	ROCCSD(T)	UCCSD(T)	description
μ_a	−0.1908	−0.1832	−0.1871	−0.1844	
μ_b					
$|\mu_a|$	0.1908	0.1832	0.1871	0.1844	
A_e	37 353.86	37 353.83	35 921.12	35 920.68	
B_e	5040.82	5040.82	5023.66	5023.01	
C_e	4441.45	4441.45	4407.29	4406.78	
Δ_J			0.1886×10^{-2}	0.1887×10^{-2}	
Δ_K			0.2392	0.2392	
Δ_{JK}			0.2579×10^{-1}	0.2584×10^{-1}	
δ_J			0.2545×10^{-3}	0.2545×10^{-3}	
δ_K			0.1947×10^{-1}	0.1950×10^{-1}	
ω_1 (a_1)	3238.4 (1.6)	3238.7 (1.7)	3238.6 (1.6)	3238.6 (1.6)	C−H stretch
ω_2 (a_1)	1620.3 (18.7)	1620.3 (18.7)	1577.1 (15.7)	1577.1 (15.7)	C−C−C stretch
ω_3 (a_1)	876.9 (35.2)	876.8 (35.4)	825.9 (29.1)	825.8 (29.1)	C−C stretch
ω_4 (a_1)	451.9 (106.1)	451.9 (106.0)	463.9 (94.2)	463.8 (94.2)	Mg−C$_2$ stretch
ω_5 (b_1)	886.6 (1.2)	887.0 (1.2)	862.5 (1.3)	862.4 (1.3)	C−H wagging (out of plane)
ω_6 (b_1)	232.4 (8.1)	232.9 (8.0)	225.9 (6.5)	225.9 (6.5)	C−C−C twist (out of plane)
ω_7 (b_2)	1346.8 (5.6)	1347.0 (5.6)	1329.9 (4.6)	1329.9 (4.6)	CCC bend (in plane)
ω_8 (b_2)	1007.2 (9.9)	1007.4 (9.9)	1010.7 (10.7)	1010.7 (10.7)	C−H wagging (in plane)
ω_9 (b_2)	271.5 (60.3)	271.6 (60.2)	287.6 (52.2)	287.4 (52.2)	CCMg bend (in plane)

[a]Centrifugal distortion constants are from the *A*-reduced Hamiltonian.

Table 4. Inertial Axis Dipole Moment Components, Absolute Dipole Moment (in Debye), Rotational and Centrifugal Distortion Constants (in MHz), Harmonic Vibrational Frequencies (in cm^{-1}), and IR Intensities (in Parentheses, in km mol^{-1}) of the $^4\Sigma^+$ Electronic State of Isomer 10 Calculated at Different Levels

parameter	6-311++G(2d,2p)		cc-pVTZ		description
	ROωB97XD	UωB97XD	ROCCSD(T)	UCCSD(T)	
μ_a	1.7020	1.6977	1.5565	1.5837	
μ_b					
$|\mu_a|$	1.7020	1.6977	1.5565	1.5837	
B_e	2396.12	2390.48	2359.18	2359.85	
D_J			0.2704×10^{-3}	0.2694×10^{-3}	
D_K			0.2704×10^{-3}	0.2694×10^{-3}	
D_{JK}			-0.5408×10^{-3}	-0.5387×10^{-3}	
$\omega_1\ (\sigma_g^+)$	3460.9 (78.1)	3451.8 (70.8)	3439.8 (74.5)	3445.4 (76.2)	C−H stretch
$\omega_2\ (\sigma_g^+)$	1664.5 (0.5)	1661.8 (4.9)	1618.5 (2.1)	1661.1 (4.7)	C−C stretch
$\omega_3\ (\sigma_g^+)$	1270.8 (41.0)	1322.3 (40.6)	1283.5 (36.2)	1288.3 (36.2)	C−C−Mg stretch
$\omega_4\ (\sigma_g^+)$	439.4 (99.0)	439.0 (97.3)	438.3 (84.4)	439.2 (83.8)	C−Mg stretch
$\omega_5\ (\pi)$	455.6 (5.7)	449.5 (0.3)	556.8 (39.5)	444.7 (0.7)	C−C−H bend
$\omega_6\ (\pi)$	439.2 (49.5)	292.9 (52.1)	507.9 (4.9)	183.0 (46.1)	C−C−H bend
$\omega_7\ (\pi)$	119.1 (11.5)	118.5 (10.9)	123.3 (20.1)	114.3 (7.6)	C−C−Mg bend

Table 5. Inertial Axis Dipole Moment Components, Absolute Dipole Moment (in Debye), Rotational and Centrifugal Distortion Constants (in MHz), Harmonic Vibrational Frequencies (in cm^{-1}), and IR Intensities (in Parentheses, in km mol^{-1}) of $^2A'$ Electronic State of Isomer 2 Calculated at Different Levels[a]

parameter	6-311++G(2d,2p)		cc-pVTZ		description
	ROωB97XD	UωB97XD	ROCCSD(T)	UCCSD(T)	
μ_a	−3.9832	3.9723	3.1792	3.1531	
μ_b	−1.9716	−1.9572	2.6699	2.6659	
$|\mu_a|$	4.4444	4.4284	4.1516	4.1291	
A_e	36 269.11	36 269.12	35 529.29	35 543.24	
B_e	3730.78	3730.78	3718.44	3722.60	
C_e	3382.81	3382.81	3366.15	3369.68	
D_J			0.5380×10^{-2}	0.7064×10^{-2}	
D_K			−0.5034	−0.9187	
D_{JK}			0.6839	1.1186	
D_1			-0.5432×10^{-3}	-0.7347×10^{-3}	
D_2			-0.4687×10^{-3}	-0.7684×10^{-3}	
$\omega_1\ (a')$	3231.7 (4.07)	3231.7 (4.0)	3227.0 (4.5)	3227.4 (4.5)	C−H stretch
$\omega_2\ (a')$	1640.7 (9.8)	1639.9 (8.2)	1606.5 (13.6)	1607.3 (13.5)	C=C stretch
$\omega_3\ (a')$	1302.3 (22.2)	1301.6 (23.7)	1281.1 (15.0)	1281.2 (15.0)	C−C−H bend
$\omega_4\ (a')$	976.7 (10.0)	975.5 (10.5)	947.6 (9.8)	947.8 (9.7)	CCC bend
$\omega_5\ (a')$	940.8 (19.1)	941.1 (18.7)	925.4 (17.6)	925.7 (17.8)	C−H wag (in plane)
$\omega_6\ (a')$	411.3 (50.5)	410.4 (48.6)	426.8 (46.5)	427.4 (46.5)	C−Mg bend
$\omega_7\ (a')$	87.9 (15.8)	88.4 (15.5)	45.6 (15.2)	38.9 (15.3)	C$_3$H kink
$\omega_8\ (a'')$	891.7 (6.0)	892.0 (6.1)	868.0 (6.2)	867.8 (6.2)	C−H wag (out of plane)
$\omega_9\ (a'')$	216.2 (0.1)	216.1 (0.0)	208.7 (0.1)	207.7 (0.2)	CCMg bend (out of plane)

[a]Centrifugal distortion constants are from the S-reduced Hamiltonian.

10 are unreliable. Thus, we rely on coupled-cluster data and other levels of theory for the relative energy of this isomer.

From the thermodynamic stability point of view, the quartet of isomer 10 is the second-most-stable isomer because it lies 8.0 kcal mol^{-1} above the doublet of 1. The doublet of isomer 2 is the third-most-stable isomer because it lies at 8.6 kcal mol^{-1} above 1. Therefore, further emphasis is mostly given to these three molecules (doublets of 1 and 2 and a quartet of 10) instead of all low-lying isomers. It is noted here that, among the doublets, geometry 8 is a transition state and all others are minima at the ROCCSD(T)/cc-pVTZ level. In the case of quartets, geometry optimization of isomers 3 and 4 leads to isomer 10, whereas isomer 9 geometry optimization leads to

isomer 8. Therefore, in total, merely eight stationary points were found within the quartet electronic states.

On the basis of the multireference characteristics of C$_3$H isomers discussed elsewhere,[65] we suspected that some of the isomers of MgC$_3$H may have multireference characteristics. To clarify this, we have computed the T_1 diagnostic values[88] for all isomers at the UCCSD/6-311++G(2d,2p)//UωB97XD/6-311++G(2d,2p) level. Calculated T_1 diagnostic values for isomers 1, 2, 5, and 11 were 0.013, 0.014, 0.019, and 0.017, respectively. Because these values are less than 0.020, one can state that these isomers are not multireference in character. For isomer 7, the value obtained was 0.022, which is slightly above the threshold. For isomers 3, 4, 6, 8, 9, and 10, the calculated T_1 values were 0.118, 0.162, 0.052, 0.139, 0.141, and 0.058,

respectively. The quartet of isomer **10** also shows moderate multireference character with a T_1 value of 0.039. Although we have not carried out multireference coupled-cluster (MRCC) or complete active space self-consistent field calculations on any of these isomers, we note that such a study is deferred to future work.

MgC_3H^+. The relative stabilities of both singlet and triplet electronic states of MgC_3H^+ isomers ($1^+–11^+$) have been calculated at different levels, and they are collected in Table 2. Like the doublet neutral radicals, on the cation PES, the singlet electronic state of 2-magnesabicyclo[1.1.0]but-1,3,4-triyl (1^+) is the most stable isomer. The singlets of isomers 2^+, 3^+, and 4^+ are 15.6, 19.6, and 21.4 kcal mol^{-1} above the singlet of 1^+, respectively, at the CCSD(T)/cc-pVTZ level. The singlet linear isomer, 10^+, is a fourth-order saddle point, and isomer 5^+ turned out to be a transition state at the latter level. Geometry optimization of 8^+ and 9^+ at all levels led to 1^+. All of the stationary points on the cation PES had higher polarity due to the positive charge. The dipole moment values of the first four isomers ($1^+–4^+$) are 7.84, 12.32, 7.32, and 7.93 D, respectively. Therefore, apart from neutrals, the cations are also suitable candidates for microwave spectroscopic and radioastronomical studies. It is noted here that the triplet electronic states of all cations are above the singlet electronic state of 1^+.

2-Magnesabicyclo[1.1.0]but-1,3,4-triyl (1). The point-group symmetry of **1** is C_{2v}, and the ground electronic state is $^2A_1$. The quartet electronic state ($^4B_1$) of **1** is a second-order saddle point and is 83.1 kcal mol^{-1} above the doublet of **1**. Though the former is energetically the most stable molecule for MgC_3H at all levels studied here, it remains elusive in the laboratory to date. The binding energy (BE) for **1** (BE = $E_{MgC_3H} - (E_{c-C_3H} + E_{Mg})$) is -47.2 kcal mol^{-1} at the (U)ωB97XD/6311++G(2d,2p) level of theory. Therefore, the molecule is sufficiently bound and the Mg–C bonds are not extremely weak. The transannular C–C bond length obtained at all levels (1.53 to 1.54 Å) reveals that it exhibits single-bond characteristics. Therefore, resonance structure **1a** is more dominant than **1b** (see Figure 4). Though isomer **1** is less polar ($\mu = 0.19$ D), in principle, it can be identified through rotational spectroscopy. We note that there are weakly polar van der Waals complexes such as the Ne–Ar dimer whose dipole moment is just 0.0022 D, yet pure rotational transitions have been measured.[94] Equilibrium rotational constants A_e, B_e, and C_e obtained from the optimized geometries at different

levels (see Table 3) reveal that this molecule is an asymmetric top. In addition, one can also detect isomer **1** through IR spectroscopy. Although two of the low-frequency modes ν_9 (287.6 cm^{-1}, CCMg bending) and ν_4 (463.9 cm^{-1}, Mg–C$_2$ stretching) are very intense, one cannot confirm these modes easily. On the other hand, ν_8 (1010.7 cm^{-1}, C–H wagging) and ν_2 (1577.0 cm^{-1}, CCC stretching) modes could readily be seen (see Table 3).

1-Magnesabutatrienyl (10). The ground electronic state of **10** is $^4\Sigma^+$. It lies 8.0 kcal mol^{-1} above **1** of the doublet at the ROCCSD(T)/cc-pVTZ level. This $C_{\infty v}$-symmetric linear molecule is the second-most-stable isomer for MgC_3H, and it is ~8 times polar than **1** with a dipole moment value of 1.56 D. However, this molecule also remains elusive in the laboratory to date. The binding energy (BE) for **10** (BE = $E_{MgC_3H} - (E_{l-C_3H} + E_{Mg})$) is -45.4 kcal mol^{-1} at the (U)ωB97XD/6-311++G(2d,2p) level of theory. This implies that the Mg atom is sufficiently bound to the carbon atom. The BE values we have calculated for isomers **1** and **10** indirectly support the relative energy ordering we have obtained for these two isomers because the most stable isomer has the highest binding energy. Six different valence structures are shown in Figure 4 for isomer **10**. Three structures (**10a**, **10c**, and **10e**) represent the quartet electronic state and the other three (**10b**, **10d**, and **10f**) represent the doublet electronic state. On the basis of the bond lengths obtained, it is evident that valence structure **10a** is dominant because the C–C bond length of 1.26 Å (connected to the H atom) exhibits triple-bond characteristics whereas the other C–C bond length is intermediate between a double and a triple bond. The rotational and centrifugal distortion constants obtained at various levels are shown in Table 4. The C–H stretching (ν_1) and C–C–Mg stretching (ν_3) modes whose frequencies are 3439.8 and 1283.5 cm^{-1}, respectively, at the ROCCSD(T)/cc-pVTZ level could readily be seen in the IR spectra.

Magnesium-Substituted Cyclopropenylidene (2). The point-group symmetry of **2** is C_s, and the ground electronic state is $^2A'$. This molecule is 8.6 kcal mol^{-1} above the doublet of **1** and is the third-most-stable isomer on the MgC_3H potential energy surface. The quartet electronic state ($^4A''$) of **2** is also a minimum, but it lies 53.0 kcal mol^{-1} above **1**. Among the three low-lying minima, isomer **2** is the highest polar molecule with a dipole moment value of 4.15 D at the ROCCSD(T)/cc-pVTZ level. Therefore, the chances of identifying this molecule both in the laboratory and in the ISM are high. Moreover, the inertial axis dipole moment components are in two directions for this molecule (see Table 5), and thus both a- and b-type rotational transitions are possible. Moreover, from equilibrium rotational constants A_e, B_e, and C_e, one could infer that this molecule is closely approaching the prolate limit because the difference between the B_e and C_e rotational constants is not very high. The C=C stretching (ν_2) and CCH bending (ν_3) modes whose frequencies are 1606.5 and 1281.1 cm^{-1}, respectively, at the ROCCSD(T)/cc-pVTZ level could readily be seen in the IR spectra.

Other Low-Lying Isomers of $MgC_3H^{0/+}$. Apart from the doublet electronic states of isomers **1** and **2** and the quartet electronic state of isomer **10**, the doublet electronic states of isomers **3**, **4**, and **5** of MgC_3H could be considered to be low-lying isomers based on the relative energies (below 30 kcal mol^{-1}). Except **5**, which is less polar, the other three isomers
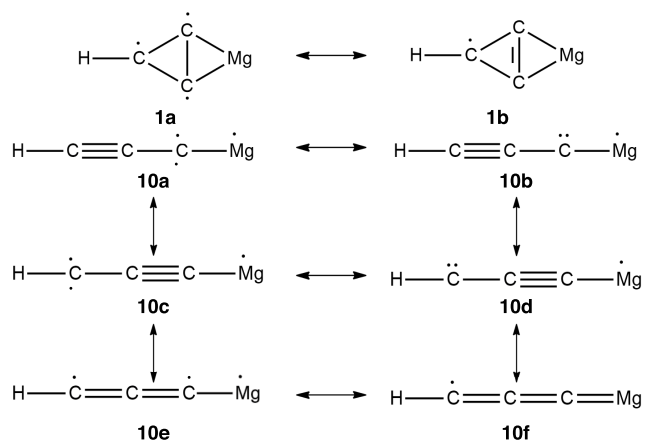

Figure 4. Valence structures of isomers **1** and **10** of MgC_3H.

are quite polar. Likewise, for the cation, apart from singlet 1^+, the three other singlet isomers (2^+-4^+) could be considered to be low-lying isomers. Therefore, the chances of identifying these molecules both in the laboratory and in the ISM are moderate.

Isomerization Pathways. To assess the kinetic stability of the low-lying doublet ($1-4$) and quartet (10 and 11) isomers, transition states have been identified initially at the UωB97XD/6-311++G(2d,2p) level, and the minimum-energy pathways are confirmed through IRC calculations at the same level. To accurately determine the activation energy barriers, single-point energy calculations are carried out at the UCCSD(T)/6-311++G(2d,2p)//UωB97XD/6-311++G-(2d,2p) level. In Figures 5–7, a schematic outline of the
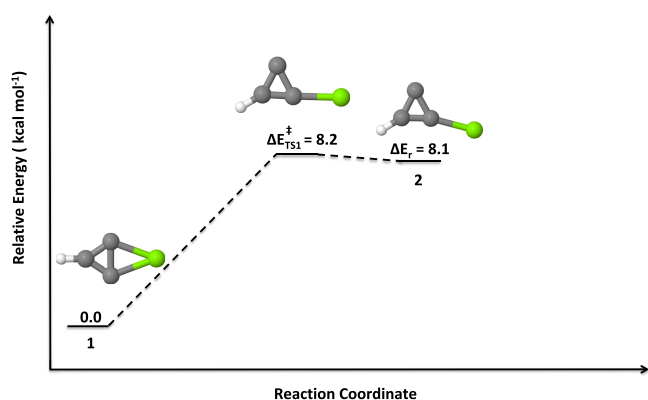
Figure 5. Isomerization pathway of isomer **1** to **2** (doublets). Relative energies are calculated at the UCCSD(T)/6-311++G-(2d,2p)//UωB97XD/6-311++G(2d,2p) level.
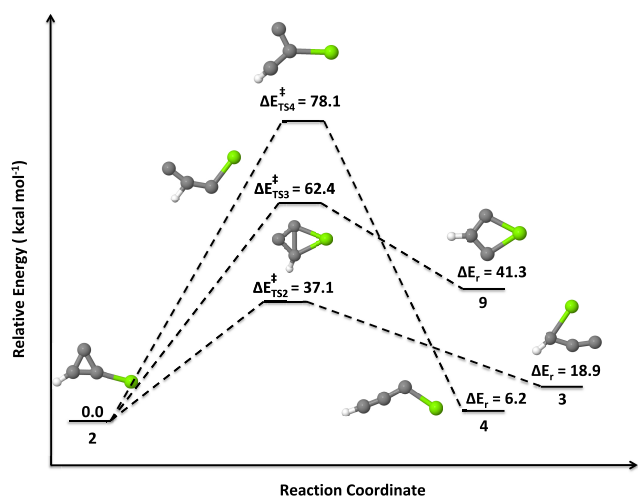
Figure 6. Isomerization pathway of isomer **2** to others (**3**, **4**, and **9**; doublets). Relative energies are calculated at the UCCSD(T)/6-311++G(2d,2p)//UωB97XD/6-311++G(2d,2p) level.

isomerization pathways of isomers **1** to **2**, **2** to **3** (as well as **4** and **9**), and **10** to **11**, respectively, is shown. Altogether, five different transition states (**TS1–TS5**) have been identified. The dissociation of the C–Mg bond (either one) of **1** leads to **TS1** with an activation energy of 8.2 kcal mol^{-1}. The reaction energy calculated for the isomerization of **1** to **2** is just 8.1 kcal mol^{-1}. This indirectly implies that the reverse process (**2** to **1**)
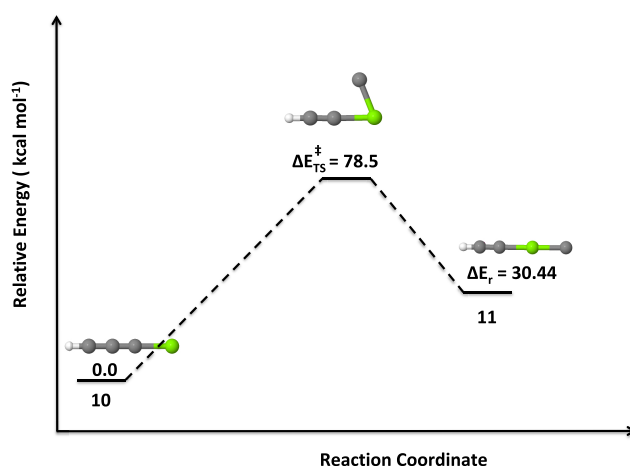

Figure 7. Isomerization pathway of isomer **10** to **11** (quartets). Relative energies are calculated at the UCCSD(T)/6-311++G-(2d,2p)//UωB97XD/6-311++G(2d,2p) level.

is nearly barrierless. Therefore, isomer **1** is certainly a kinetically stable molecule.

For the isomerization of **2**, three different transition states (**TS2**, **TS3**, and **TS4**; see Figure 6) have been identified. By bringing the C–Mg bond closer to the carbene carbon of **2**, one could get a puckered four-membered transition state with a trans-annular C–C bond. The activation energy for **TS2** is 37.1 kcal mol^{-1}. IRC calculations from this lead to isomer **3** with a reaction energy of 18.9 kcal mol^{-1}. We also identified two more transition states by breaking the C–C single bonds of the cyclopropenylidene ring of **2**. The activation energies for **TS3** and **TS4** are 62.4 and 78.1 kcal mol^{-1}, respectively. These are high-energy transition states; therefore, the conversions of **2** to **9** and **2** to **4** are unlikely to occur. The isomerization of **2** to **3** is also unlikely because it requires an activation of energy of 37.1 kcal mol^{-1}. However, isomerization of **2** to **1** is barrierless and thus **2** is not a kinetically stable molecule. Next, we turned our attention to the low-lying quartet isomers (**10** and **11**) because the quartet of isomer **10** is the second-most-stable molecule thermodynamically. It is also worth mentioning here that among the quartets, isomer **10** is the most stable molecule. Bending of the C–Mg bond of **10** leads to **TS5** and thus the isomerization of **10** to **11** requires an activation energy of 78.5 kcal mol^{-1}, which is quite high. Therefore, we conclude that the quartet linear isomer of **10** is not only a thermodynamically stable but also a kinetically stable molecule.

***Ab Initio* Molecular Dynamics.** Apart from identifying transition-state geometries and confirming the minimum-energy paths through IRC calculations, we have also carried out *ab initio* molecular dynamics simulations to reaffirm the kinetic stability of two of the lowest lying isomers of MgC$_3$H (a doublet of **1** and a quartet of **10**). These calculations were made using the ADMP[89] approach as incorporated in the Gaussian 16 program.[90] These simulations were carried out at 298 K and 1 atm pressure for 10 000 fs. For isomers **1** and **10**, the time evolutions of total energies are shown in Figures 8 and 9, respectively. To show the geometric changes that are happening to each isomer over 10 000 fs, snapshots at 2000 fs interval are added. These figures show a balanced oscillation in the energies and also firmness in the geometries over the entire time period. Therefore, one can further conclude that these molecules are indeed kinetically stable.
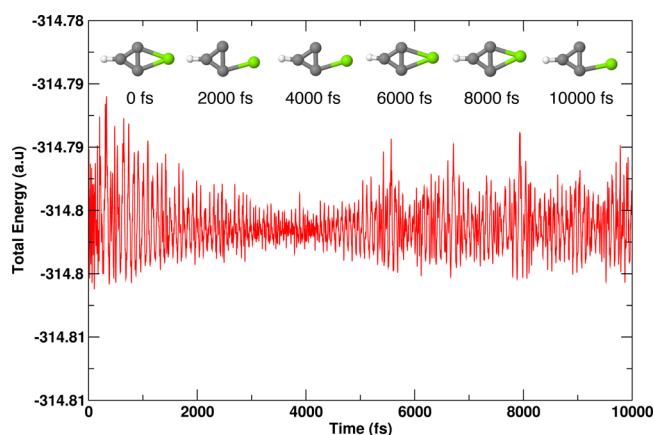
Figure 8. Energy evolution of isomer **1** ($^2A_1$) of MgC_3H obtained from the AIMD simulation carried out at 298 K and 1 atm pressure for 10 000 fs at the $U\omega B97XD/6\text{-}311\text{++}G(2d,2p)$ level.
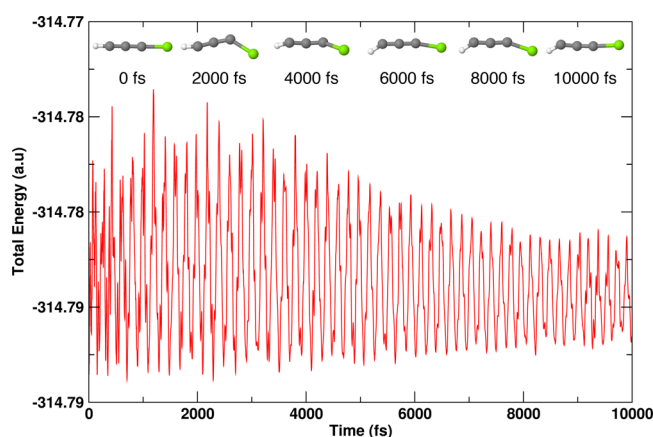

Figure 9. Energy evolution of isomer **10** ($^4\Sigma^+$) of MgC_3H obtained from the AIMD simulation carried out at 298 K and 1 atm pressure for 10 000 fs at the $U\omega B97XD/6\text{-}311\text{++}G(2d,2p)$ level.

CONCLUSIONS

Various isomers of $MgC_3H^{0/+}$ are studied in this work, which are systems of potential interstellar interest, by using DFT, coupled-cluster, and thermochemical modules. For both $MgC_3H^{0/+}$, the most stable isomer turns out to be isomer **1** (1^+), which is a cyclic molecule. This is a stark contrast compared to the even-numbered MgC_nH isomers ($n = 2, 4$, etc.), where the most stable isomers are linear molecules. Linear isomer **10** within the quartet electronic state ($^4\Sigma^+$) was found to be the second-most-stable isomer thermodynamically at various levels. Though the doublet of **10** turns out to be a minimum at the $ROCCSD(T)/cc\text{-}pVTZ$ level, it lies 54.1 kcal mol^{-1} above the doublet electronic state of **1**. The doublet of **10** is certainly the most polar molecule with a dipole moment of 7.90 D. However, it lies in the high-energy region. Considering the presence of cyclic-C_3H, linear-C_3H, and Mg^+ in the ISM, it is postulated here that the formation of isomers **1** and **10** is plausible. Though isomer **1** is less polar ($\mu = 0.19$ D), the detection of **1** in the laboratory should be possible. On the other hand, the quartet electronic state of isomer **10** is moderately polar ($\mu = 1.55$ D). Therefore, identifying isomer **10** in the laboratory may be more straightforward than identifying isomer **1**. Among the three low-lying minima, isomer **2** is highly polar with a dipole

moment value of 4.15 D. However, **2** is not kinetically stable at all because the isomerization pathway of **1** to **2** indicates that it will quickly revert back to **1**. Therefore, the detection of this molecule in the laboratory will be very challenging. It is also noted here that the doublet electronic states of isomers **3**, **4**, and **6** are quite polar with dipole moments of 7.45, 3.04, and 4.38 D, respectively. Therefore, the detection of these molecules is also possible though they are on the high-energy side. Isomerization pathways indicate that the three low-lying isomers (doublets of **1** and **4** and a quartet of **10**) are kinetically stable molecules. For MgC_3H^+, the cyclic isomers (1^+, 2^+, and 3^+) are on the low-energy side. The singlet linear isomer, 10^+, turned out to be a fourth-order saddle point at the $CCSD(T)/cc\text{-}pVTZ$ level. Moreover, the low-lying cations are quite polar with dipole moment values of >7.00 D. Therefore, they are also suitable candidates for laboratory detection by rotational spectroscopy. To conclude, the structural, energetic, and rotational spectroscopic parameters computed in this work would aid both molecular spectroscopists and radioastronomers in the future.

ASSOCIATED CONTENT

Supporting Information

The Supporting Information is available free of charge at https://pubs.acs.org/doi/10.1021/acs.jpca.2c02220.

> Cartesian coordinates of the optimized geometries, total electronic energies, and zero-point vibrational energies calculated at different levels; optimal geometry parameters obtained from DFT, harmonic vibrational frequencies, infrared intensities, and anharmonic vibrational frequencies for two of the low-lying isomers (PDF)

AUTHOR INFORMATION

Corresponding Author

Venkatesan S. Thimmakondu − *Department of Chemistry and Biochemistry, San Diego State University, San Diego, California 92182-1030, United States;* ◉ orcid.org/0000-0002-7505-077X; Email: vthimmakondusamy@sdsu.edu

Authors

Sunanda Panda − *Department of Chemistry, Indian Institute of Technology Kharagpur, Kharagpur 721 302 West Bengal, India*

Devipriya Sivadasan − *Department of Chemistry, School of Advanced Sciences, Vellore Institute of Technology, Vellore 632 014 Tamil Nadu, India*

Nisha Job − *Department of Chemistry, School of Advanced Sciences, Vellore Institute of Technology, Vellore 632 014 Tamil Nadu, India;* ◉ orcid.org/0000-0003-3103-568X

Aland Sinjari − *School of Mathematics, Biological, Exercise & Physical Sciences, San Diego Miramar College, San Diego, California 92126-2910, United States*

Krishnan Thirumoorthy − *Department of Chemistry, School of Advanced Sciences, Vellore Institute of Technology, Vellore 632 014 Tamil Nadu, India;* ◉ orcid.org/0000-0003-0920-4547

Anakuthil Anoop − *Department of Chemistry, Indian Institute of Technology Kharagpur, Kharagpur 721 302 West Bengal, India;* ◉ orcid.org/0000-0002-8116-5506

Complete contact information is available at:
https://pubs.acs.org/10.1021/acs.jpca.2c02220

Notes

■ REFERENCES

(1) Shimizu, M. Origin of Interstellar Molecules. *Prog. Theor. Phys.* **1973**, *49*, 153−164.

(2) Herbst, E. The chemistry of interstellar space. *Chem. Soc. Rev.* **2001**, *30*, 168−176.

(3) Herbst, E.; van Dishoeck, E. F. Complex Organic Interstellar Molecules. *Annu. Rev. Astron. Astrophys.* **2009**, *47*, 427−480.

(4) Klemperer, W. Interstellar chemistry. *Proc. Natl. Acad. Sci. U.S.A* **2006**, *103*, 12232−12234.

(5) Etim, E. E.; Arunan, E. Interstellar Isomeric Species: Energy, Stability and Abundance Relationship. *Eur. Phys. J. Plus* **2016**, *131*, 448.

(6) Ziurys, L. M. The Chemistry in Circumstellar Envelopes of Evolved Stars: Following the Origin of the Elements to the Origin of Life. *Proc. Natl. Acad. Sci. U.S.A* **2006**, *103*, 12274−12279.

(7) Redondo, P.; Barrientos, C.; Largo, A. Complex Organic Molecules Formation in Space Through Gas Phase Reactions: A Theoretical Approach. *Astrophys. J.* **2017**, *836*, 240.

(8) Thimmakondu, V. S.; Karton, A. Energetic and Spectroscopic Properties of the Low-Lying C_7H_2 Isomers: A High-Level Ab Initio Perspective. *Phys. Chem. Chem. Phys.* **2017**, *19*, 17685−17697.

(9) Karton, A.; Thimmakondu, V. S. From Molecules with a Planar Tetracoordinate Carbon to an Astronomically Known C_5H_2 Carbene. *J. Phys. Chem. A* **2022**, *126*, 2561−2568.

(10) McCarthy, M. C.; Travers, M. J.; Kovács, A.; Chen, W.; Novick, S. E.; Gottlieb, C. A.; Thaddeus, P. Detection and Characterization of the Cumulene Carbenes H_2C_5 and H_2C_6. *Science* **1997**, *275*, 518−520.

(11) Vrtilek, J. M.; Gottlieb, C. A.; Thaddeus, P. Laboratory and Astronomical Spectroscopy of C_3H_2, the First Interstellar Organic Ring. *Astrophys. J.* **1987**, *314*, 716.

(12) Vrtilek, J. M.; Gottlieb, A.; Gottlieb, E. W.; Killian, T. C.; Thaddeus, P. Laboratory Detection of Propadienylidene H_2CCC. *Astrophys. J.* **1990**, *364*, L53−L56.

(13) Killian, T. C.; Vrtilek, J. M.; Gottlieb, C. A.; Gottlieb, E. W.; Thaddeus, P. Laboratory Detection of A Second Carbon Chain Carbene - Butatrienylidene, H_2CCCC. *Astrophys. J.* **1990**, *365*, L89−L92.

(14) Fulara, J.; Freivogel, P.; Forney, D.; Maier, J. P. Electronic Absorption Spectra of Linear Carbon Chains in Neon Matrices. III. $HC_{2n+1}H$. *J. Chem. Phys.* **1995**, *103*, 8805−8810.

(15) Seburg, R. A.; Patterson, E. V.; Stanton, J. F.; McMahon, R. J. Structures, Automerizations, and Isomerizations of C_3H_2 Isomers. *J. Am. Chem. Soc.* **1997**, *119*, 5847−5856.

(16) Travers, M. J.; McCarthy, M. C.; Gottlieb, C. A.; Thaddeus, P. Laboratory Detection of the Ring-Chain Molecule C_5H_2. *Astrophys. J.* **1997**, *483*, L135−L138.

(17) Gottlieb, C. A.; McCarthy, M. C.; Gordon, V. D.; Chakan, J. M.; Apponi, A. J.; Thaddeus, P. Laboratory Detection of Two New C_5H_2 Isomers. *Astrophys. J.* **1998**, *509*, L141.

(18) Blanksby, S. J.; Dua, S.; Bowie, J. H.; Schröder, D.; Schwarz, H. Gas-Phase Syntheses of Three Isomeric C_5H_2 Radical Anions and Their Elusive Neutrals. A Joint Experimental and Theoretical Study. *J. Phys. Chem. A* **1998**, *102*, 9949−9956.

(19) Bowling, N. P.; Halter, R. J.; Hodges, J. A.; Seburg, R. A.; Thomas, P. S.; Simmons, C. S.; Stanton, J. F.; McMahon, R. J. Reactive Carbon-Chain Molecules: Synthesis of 1-Diazo-2,4-penta-diyne and Spectroscopic Characterization of Triplet Pentadiynylidene (H-C-C-C̈-C-C-H). *J. Am. Chem. Soc.* **2006**, *128*, 3291−3302.

(20) Steglich, M.; Fulara, J.; Maity, S.; Nagy, A.; Maier, J. P. Electronic Spectra of Linear HC_5H and Cumulene Carbene H_2C_5. *J. Chem. Phys.* **2015**, *142*, 244311.

(21) Stanton, J. F.; Garand, E.; Kim, J.; Yacovitch, T. I.; Hock, C.; Case, A. S.; Miller, E. M.; Lu, Y.-J.; Vogelhuber, K. M.; Wren, S. W.; et al. Ground and Low-Lying Excited States of Propadienylidene ($H_2C{=}C{=}C{:}$) Obtained by Negative Ion Photoelectron Spectroscopy. *J. Chem. Phys.* **2012**, *136*, 134312.

(22) McGuire, B. A.; Burkhardt, A. M.; Shingledecker, C. N.; Kalenskii, S. V.; Herbst, E.; Remijan, A. J.; McCarthy, M. C. Detection of Interstellar HC_5O in TMC-1 with the Green Bank Telescope. *Astrophys. J. Lett.* **2017**, *843*, L28.

(23) Roy, T.; Ghosal, S.; Thimmakondu, V. S. Six Low-Lying Isomers of $C_{11}H_8$ Are Unidentified in the Laboratory - A Theoretical Study. *J. Phys. Chem. A* **2021**, *125*, 4352−4364.

(24) Fulara, J.; Nagy, A.; Filipkowski, K.; Thimmakondu, V. S.; Stanton, J. F.; Maier, J. P. Electronic Transitions of $C_6H_4^+$ Isomers: Neon Matrix and Theoretical Studies. *J. Phys. Chem. A* **2013**, *117*, 13605−13615.

(25) Thirumoorthy, K.; Viji, M.; Pandey, A. P.; Netke, T. G.; Sekar, B.; Yadav, G.; Deshpande, S.; Thimmakondu, V. S. Many Unknowns Below or Close to the Experimentally Known Cumulene Carbene - A Case Study of C_9H_2 Isomers. *Chem. Phys.* **2019**, *527*, 110496.

(26) Martin-Drumel, M.-A.; Baraban, J. H.; Changala, P. B.; Stanton, J. F.; McCarthy, M. C. The Hunt for Elusive Molecules: Insights from Joint Theoretical and Experimental Investigations. *Chem: - Eur. J.* **2019**, *25*, 7243−7258.

(27) Thirumoorthy, K.; Karton, A.; Thimmakondu, V. S. From High-Energy C_7H_2 Isomers with A Planar Tetracoordinate Carbon Atom to An Experimentally Known Carbene. *J. Phys. Chem. A* **2018**, *122*, 9054−9064.

(28) Thimmakondu, V. S.; Ulusoy, I.; Wilson, A. K.; Karton, A. Theoretical Studies of Two Key Low-Lying Carbenes of C_5H_2 Missing in the Laboratory. *J. Phys. Chem. A* **2019**, *123*, 6618−6627.

(29) Reddy, S. N.; Mahapatra, S. Theoretical Study on Molecules of Interstellar Interest. II. Radical Cation of Compact Polycyclic Aromatic Hydrocarbons. *J. Phys. Chem. B* **2015**, *119*, 11391−11402.

(30) Job, N.; Karton, A.; Thirumoorthy, K.; Cooksy, A. L.; Thimmakondu, V. S. Theoretical Studies of SiC_4H_2 Isomers Delineate Three Low-Lying Silylidenes Are Missing in the Laboratory. *J. Phys. Chem. A* **2020**, *124*, 987−1002.

(31) Thimmakondu, V. S.; Karton, A. The Quest for the Carbene Bent-pentadiynylidene Isomer of C_5H_2. *Chem. Phys.* **2018**, *515*, 411−417.

(32) He, C.; Galimova, G. R.; Luo, Y.; Zhao, L.; Eckhardt, A. K.; Sun, R.; Mebel, A. M.; Kaiser, R. I. A Chemical Dynamics Study on the Gas-Phase Formation of Triplet and Singlet C_5H_2 Carbenes. *Proc. Natl. Acad. Sci. U. S. A.* **2020**, *117*, 30142−30150.

(33) Levey, Z. D.; Laws, B. A.; Sundar, S. P.; Nauta, K.; Kable, S. H.; da Silva, G.; Stanton, J. F.; Schmidt, T. W. PAH Growth in Flames and Space: Formation of the Phenalenyl Radical. *J. Phys. Chem. A* **2022**, *126*, 101−108.

(34) Anderson, M. A.; Ziurys, L. M. Laboratory Detection and Millimeter Spectrum of the MgCCH Radical. *Astrophys. J.* **1995**, *439*, L25.

(35) Brewster, M.; Apponi, A.; Xin, J.; Ziurys, L. Millimeter-Wave Spectroscopy of Vibrationally-Excited NaCCH $(\tilde{X}^1\Sigma^+)$ and MgCCH $(\tilde{X}^2\Sigma^+)$: The ν_5 Bending Mode. *Chem. Phys. Lett.* **1999**, *310*, 411−422.

(36) Guélin, M.; Lucas, R.; Cernicharo, J. MgNC and the Carbon-Chain Radicals in IRC+10216. *Astron. Astrophys.* **1993**, *280*, L19−L22.

(37) Ziurys, L. M.; Apponi, A. J.; Guélin, M.; Cernicharo, J. Detection of MgCN in IRC+10216: A New Metal Bearing Free Radical. *Astrophys. J.* **1995**, *445*, L47.

(38) Woon, D. E. Ab Initio Characterization of MgCCH, MgCCH$^+$, and MgC$_2$ and Pathways to Their Formation in the Interstellar Medium. *Astrophys. J.* **1996**, *456*, 602.

(39) Woon, D. E. A. Correlated Ab Initio Study of the $\tilde{A}^2\Pi\leftarrow \tilde{X}^2\Sigma^+$ Transition in MgCCH. *Chem. Phys. Lett.* **1997**, *274*, 299.

(40) Agundez, M.; Cernicharo, J.; Guelin, M. New Molecules in IRC +10216: Confirmation of C$_5$S and Tentative Identification of MgCCH, NCCP, and SiH$_3$CN. *Astron. Astrophys.* **2014**, *570*, A45.

(41) Cernicharo, J.; Cabezas, C.; Pardo, J. R.; Agúndez, M.; Bermúdez, C.; Velilla-Prieto, L.; Tercero, F.; López-Pérez, J. A.; Gallego, J. D.; Fonfría, J. P.; et al. Discovery of Two New Magnesium-Bearing Species in IRC+10216: MgC$_3$N and MgC$_4$H. *Astron. Astrophys.* **2019**, *630*, L2.

(42) Dunbar, R. C.; Petrie, S. Interstellar and Circumstellar Reaction Kinetics of Na$^+$, Mg$^+$, and Al$^+$ with Cyanopolyynes and Polyynes. *Astrophys. J.* **2002**, *564*, 792−802.

(43) Petrie, S.; Kagi, E.; Kawaguchi, K. Has MgCCCN Been Detected Within the Envelope of IRC+10216? *Mon. Not. R. Astron. Soc.* **2003**, *343*, 209.

(44) Vega-Vega, A.; Largo, A.; Redondo, P.; Barrientos, C. Structure and Spectroscopic Properties of [Mg,C,N,O] Isomers: Plausible Astronomical Molecules. *ACS Earth Space Chem.* **2017**, *1*, 158−167.

(45) Thimmakondu, V. S. MgC$_2$H$_2$ Isomers − Simple Penta-Atomic Molecules Missing in the Laboratory. *Chem. Phys.* **2020**, *538*, 110899.

(46) Pandey, A. P.; Padidela, U. K.; Thulasiraman, L. K.; Sethu, R.; Vairaprakash, P.; Thimmakondu, V. S. MgC$_6$H$_2$ Isomers: Potential Candidates for Laboratory and Radioastronomical Studies. *J. Phys. Chem. A* **2020**, *124*, 7518−7525.

(47) Ruf, A.; Kanawati, B.; Hertkorn, N.; Yin, Q.-Z.; Moritz, F.; Harir, M.; Lucio, M.; Michalke, B.; Wimpenny, J.; Shilobreeva, S.; et al. Previously Unknown Class of Metalorganic Compounds Revealed in Meteorites. *Proc. Natl. Acad. Sci. U.S.A* **2017**, *114*, 2819−2824.

(48) Bai, J.; Yu, H.-T. Theoretical Investigation of the Structures, Stabilities, and Vibrational and Rotational Spectroscopic Parameters of Linear HOMgNC and HMgNCO Molecules by Density Functional Theory and Coupled-Cluster Method. *New J. Chem.* **2022**, *46*, 7879−7891.

(49) Highberger, J. L.; Savage, C.; Bieging, J. H.; Ziurys, L. M. Heavy-Metal Chemistry in Proto-Planetary Nebulae: Detection of MgNC, NaCN, and AlF toward CRL 2688. *Astrophys. J.* **2001**, *562*, 790−798.

(50) Highberger, J. L.; Ziurys, L. M. Detection of MgNC in CRL 618: Tracing Metal Chemistry with Asymptotic Giant Branch Evolution. *Astrophys. J.* **2003**, *597*, 1065−1069.

(51) Pardo, J. R.; Cabezas, C.; Fonfría, J. P.; Agúndez, M.; Tercero, B.; de Vicente, P.; Guélin, M.; Cernicharo, J. Magnesium Radicals MgC$_5$N and MgC$_6$H in IRC + 10216. *Astron. Astrophys.* **2021**, *652*, L13.

(52) Beardah, M. S.; Ellis, A. M. Production and Detection of Short-Lived Metal-Containing Molecules in the Gas Phase: A Review. *J. Chem. Technol. and Biotechnol.* **1999**, *74*, 863−869.

(53) Ding, H.; Apetrei, C.; Chacaga, Ł.; Maier, J. P. Electronic Spectra of MgC$_{2n}$H ($n = 1−3$) Chains in the Gas Phase. *Astrophys. J.* **2008**, *677*, 348−352.

(54) Chasovskikh, E.; Jochnowitz, E. B.; Maier, J. P. Electronic Spectra of the MgC$_4$H and MgC$_6$H Radicals. *J. Phys. Chem. A* **2008**, *112*, 8686−8689.

(55) Forthomme, D.; Linton, C.; Tokaryk, D.; Adam, A.; Granger, A. High-Resolution Laser Spectroscopy of the $\tilde{A}^2\Pi−\tilde{X}^2\Sigma^+$ Transition of MgC$_4$H. *Chem. Phys. Lett.* **2010**, *488*, 116−120.

(56) Barrientos, C.; Redondo, P.; Largo, A. Ionization and Protonation of MgC$_3$: A Theoretical Study. *Int. J. Quantum Chem.* **2002**, *86*, 114−121.

(57) Redondo, P.; Barrientos, C.; Largo, A. Structures and Stabilities of MgC$_3$ Isomers: A Theoretical Study. *Chem. Phys. Lett.* **2001**, *335*, 64−70.

(58) Dong, F.; Xie, Y.; Bernstein, E. R. Experimental and Theoretical Studies of Neutral Mg$_m$C$_n$H$_x$ and Be$_m$C$_n$H$_x$ Clusters. *J. Chem. Phys.* **2011**, *135*, 054307.

(59) Bejjani, M.; Rittby, C. M. L.; Graham, W. R. M. Fourier Transform Infrared Matrix and Density Functional Theory Study of the Vibrational Spectrum of the Linear MgC$_3^-$ Anion. *J. Chem. Phys.* **2011**, *135*, 054513.

(60) Irvine, W. M. The Chemistry of Cold, Dark Interstellar Clouds. *Astrochemistry; Proceedings of the IAU Symposium*; Goa, India, Dec 3−7, 1985; Vol. 120, pp 245−252.

(61) Thaddeus, P.; Gottlieb, C. A.; Hjalmarson, A.; Johansson, L. E. B.; Irvine, W. M.; Friberg, P.; Linke, R. A. Astronomical Identification of the C$_3$H Radical. *Astrophys. J.* **1985**, *294*, L49−L53.

(62) Gottlieb, C. A.; Vrtilek, J. M.; Gottlieb, E. W.; Thaddeus, P.; Hjalmarson, A. Laboratory Detection of the C$_3$H Radical. *Astrophys. J.* **1985**, *294*, L55−L58.

(63) Yamamoto, S.; Saito, S.; Ohishi, M.; Suzuki, H.; Ishikawa, S.-I.; Kaifu, N.; Murakami, A. Laboratory and Astronomical Detection of the Cyclic-C$_3$H Radical. *Astrophys. J.* **1987**, *322*, L55.

(64) Mangum, J. G.; Wootten, A. Observations of the cyclic C$_3$H radical in the interstellar medium. *Astron. Astrophys.* **1990**, *239*, 319.

(65) Ikuta, S. An Ab Initio MO Study on Structures and Energetics of C$_3$H$^-$, C$_3$H, and C$_3$H$^+$. *J. Chem. Phys.* **1997**, *106*, 4536−4542.

(66) Thaddeus, P.; McCarthy, M. C.; Travers, M. J.; Gottlieb, C. A.; Chen, W. New Carbon Chains in the Laboratory and in Interstellar Space. *Faraday Discuss.* **1998**, *109*, 121.

(67) Ehrenfreund, P.; Charnley, S. B. Organic Molecules in the Interstellar Medium, Comets, and Meteorites: A Voyage from Dark Clouds to the Early Earth. *Annu. Rev. Astron. Astrophys.* **2000**, *38*, 427.

(68) Martin-Drumel, M.-A.; Baraban, J. H.; Changala, P. B.; Stanton, J. F.; McCarthy, M. C. The Hunt for Elusive Molecules: Insights from Joint Theoretical and Experimental Investigations. *Chem—Eur. J.* **2019**, *25*, 7243.

(69) Agúndez, M.; Cernicharo, J.; Quintana-Lacaci, G.; Castro-Carrizo, A.; Velilla Prieto, L.; Marcelino, N.; Guélin, M.; Joblin, C.; Martín-Gago, J. A.; Gottlieb, C. A. Growth of Carbon Chains in IRC +10216 Mapped with ALMA. *Astron. Astrophys.* **2017**, *601*, A4.

(70) Belloche, A.; Müller, H. S. P.; Menten, K. M.; Schilke, P.; Comito, C. Complex Organic Molecules in the Interstellar Medium: IRAM 30 m Line Survey of Sagittarius B2(N) and (M). *Astron. Astrophys.* **2013**, *559*, A47.

(71) Herbst, E.; van Dishoeck, E. F. Complex Organic Interstellar Molecules. *Annu. Rev. Astron. Astrophys.* **2009**, *47*, 427.

(72) Kaiser, R. I. Experimental Investigation on the Formation of Carbon-Bearing Molecules in the Interstellar Medium via Neutral-Neutral Reactions. *Chem. Rev.* **2002**, *102*, 1309.

(73) Snow, T. P.; McCall, B. J. Diffuse Atomic and Molecular Clouds. *Annu. Rev. Astron. Astrophys.* **2006**, *44*, 367.

(74) Woon, D. E.; Herbst, E. Quantum Chemical Predictions of the Properties of Known and Postulated Neutral Interstellar Molecules. *Astrophys. J., Suppl. Ser.* **2009**, *185*, 273.

(75) Chai, J.-D.; Head-Gordon, M. Long-Range Corrected Hybrid Density Functionals with Damped Atom−Atom Dispersion Corrections. *Phys. Chem. Chem. Phys.* **2008**, *10*, 6615−6620.

(76) Krishnan, R.; Binkley, J. S.; Seeger, R.; Pople, J. A. Self-Consistent Molecular Orbital Methods. XX. A Basis Set for Correlated Wave Functions. *J. Chem. Phys.* **1980**, *72*, 650−654.

(77) Clark, T.; Chandrasekhar, J.; Spitznagel, G. W.; Schleyer, P. V. R. Efficient Diffuse Function-Augmented Basis Sets for Anion Calculations. III. The 3-21+G Basis Set for First-Row Elements, Li-F. *J. Comput. Chem.* **1983**, *4*, 294−301.

(78) Raghavachari, K.; Trucks, G. W.; Pople, J. A.; Head-Gordon, M. A Fifth-Order Perturbation Comparison of Electron Correlation Theories. *Chem. Phys. Lett.* **1989**, *157*, 479−483.

(79) Bartlett, R. J.; Watts, J.; Kucharski, S.; Noga, J. Non-Iterative Fifth-Order Triple and Quadruple Excitation Energy Corrections In Correlated Methods. *Chem. Phys. Lett.* **1990**, *165*, 513−522.

(80) Grimme, S.; Antony, J.; Ehrlich, S.; Krieg, H. A Consistent and Accurate Ab Initio Parametrization of Density Functional Dispersion Correction (DFT-D) for the 94 Elements H-Pu. *J. Chem. Phys.* **2010**, *132*, 154104.

(81) Baboul, A. G.; Curtiss, L. A.; Redfern, P. C.; Raghavachari, K. Gaussian-3 Theory using Density Functional Geometries and Zero-Point Energies. *J. Chem. Phys.* **1999**, *110*, 7650−7657.

(82) Curtiss, L. A.; Redfern, P. C.; Raghavachari, K. Gaussian-4 Theory. *J. Chem. Phys.* **2007**, *126*, 084108.

(83) Curtiss, L. A.; Redfern, P. C.; Raghavachari, K. Gaussian-4 Theory Using Reduced Order Perturbation Theory. *J. Chem. Phys.* **2007**, *127*, 124105.

(84) Montgomery, J. A.; Frisch, M. J.; Ochterski, J. W.; Petersson, G. A. A Complete Basis Set Model Chemistry. VI. Use of Density Functional Geometries and Frequencies. *J. Chem. Phys.* **1999**, *110*, 2822−2827.

(85) Montgomery, J. A.; Frisch, M. J.; Ochterski, J. W.; Petersson, G. A. A Complete Basis Set Model Chemistry. VII. Use of the Minimum Population Localization Method. *J. Chem. Phys.* **2000**, *112*, 6532−6542.

(86) Fukui, K. The Path of Chemical Reactions - The IRC Approach. *Acc. Chem. Res.* **1981**, *14*, 363−368.

(87) Hratchian, H. P.; Schlegel, H. B. In *Theory and Applications of Computational Chemistry*; Dykstra, C. E., Frenking, G., Kim, K. S., Scuseria, G. E., Eds.; Elsevier: Amsterdam, 2005; pp 195−249.

(88) Lee, T. J.; Taylor, P. R. A diagnostic for determining the quality of single-reference electron correlation methods. *Int. J. Quantum Chem.* **1989**, *36*, 199−207.

(89) Schlegel, H. B.; Millam, J. M.; Iyengar, S. S.; Voth, G. A.; Daniels, A. D.; Scuseria, G. E.; Frisch, M. J. Ab Initio Molecular Dynamics: Propagating the Density Matrix with Gaussian Orbitals. *J. Chem. Phys.* **2001**, *114*, 9758−9763.

(90) Frisch, M. J.; Trucks, G. W.; Schlegel, H. B.; Scuseria, G. E.; Robb, M. A.; Cheeseman, J. R.; Scalmani, G.; Barone, V.; Petersson, G. A.; Nakatsuji, H. et al. *Gaussian 16*, Revision B.01; Gaussian Inc.: Wallingford, CT, 2016.

(91) Stanton, J. F.; Gauss, J.; Cheng, L.; Harding, M. E.; Matthews, D. A.; Szalay, P. G.*CFOUR, Coupled-Cluster Techniques for Computational Chemistry, A Quantum-Chemical Program Package*.   With contributions from A. A. Auer, R. J. Bartlett, U. Benedikt, C. Berger, D. E. Bernholdt, Y. J. Bomble, O. Christiansen, F. Engel, R. Faber, M. Heckert, O. Heun, M. Hilgenberg, C. Huber, T.-C. Jagau, D. Jonsson, J. Juselius, T. Kirsch, K. Klein, W. J. Lauderdale, F. Lipparini, T. Metzroth, L. A. Mück, D .P. O 'Neill, D. R. Price, E. Prochnow, C. Puzzarini, K. Ruud, F. Schimann, W. Schwalbach, C. Simmons, S. Stopkowicz, A. Tajti, J. Vazquez, F. Wang, J. D. Watts, the integral packages MOLECULE (J. Almlöf and P. R. Taylor), PROPS (P. R. Taylor), ABACUS (T. Helgaker, H. J. Aa. Jensen, P. Jorgensen, and J. Olsen), and ECP routines by A. V. Mitin and C. van Wüllen. For the current version, see http://www.cfour.de.

(92) Bauernschmitt, R.; Ahlrichs, R. Stability Analysis for Solutions of the Closed Shell Kohn−Sham Equation. *J. Chem. Phys.* **1996**, *104*, 9047−9052.

(93) Crawford, T. D.; Stanton, J. F.; Allen, W. D.; Schaefer, H. F. Hartree-Fock Orbital Instability Envelopes in Highly Correlated Single-Reference Wave Functions. *J. Chem. Phys.* **1997**, *107*, 10626−10632.

(94) Grabow, J.-U.; Pine, A. S.; Fraser, G. T.; Lovas, F. J.; Suenram, R. D.; Emilsson, T.; Arunan, E.; Gutowsky, H. S. Rotational Spectra and van der Waals Potentials of Ne-Ar. *J. Chem. Phys.* **1995**, *102*, 1181−1187.